



39 **Abstract**

40 Continuous manufacturing (CM) has been used to produce several immediate release drug products. No  
41 extended-release (ER) product manufactured employing CM technology has been approved yet. This  
42 study investigated the critical aspects of switching from the batch mode of high shear granulation to the  
43 continuous operation of twin-screw granulation for extended-release tablets. Metoprolol succinate ER  
44 tablets was used as a model ER formulation for this purpose. A central composite design (CCD) was  
45 employed to determine the effects of high shear granulator (HSG) parameters, namely impeller  
46 speed, granulation time, and binder liquid feeding rate, on the critical granulation characteristics  
47 important for product performance. These critical granulation characteristics served as a guide for  
48 switching from the batch processing to the continuous operation for achieving the same breaking  
49 strength and dissolution for this ER metoprolol tablets.

50 The granulation time was the most critical factor affecting the bulk properties of granules which  
51 contributed to tablet dissolution. The higher density and lower compressibility of granules were attained  
52 at the longest granulation time of 5.4 min with the fastest liquid feeding rate of 75 g/min. The granules'  
53 density was the primary factor negatively affecting the dissolution of metoprolol tablets. However, the  
54 breaking strength of tablets confounded the effect of granules density on metoprolol dissolution.  
55 Switching the processing parameters of high shear granulation to twin-screw granulation achieved  
56 similar dissolution profiles ( $F2 > 50$ ). The screw speed was not found to affect bulk properties of  
57 granules. The root cause of granulation failures in twin-screw granulation, such as premature  
58 consolidation, excessive swelling, poor cohesion, inconsistent shearing effects, and formation of  
59 deformed agglomerates, were identified. In conclusion, the use of critical granulation characteristics  
60 through a performance-based approach of ER tablets facilitated the switching of manufacturing of an ER  
61 formulation form batch to continuous operation.

62

63 **Keywords:** Twin-screw granulation, high-shear granulation, Continuous manufacturing, Extended-  
64 release tablets, formulation, Oral solid dosage processing, Design space

65

66

67

68

69

70

71

72

73

74

75

76

77

78 **Introduction**

79 Wet granulation (WG) is a size enlargement process in which fine powders agglomerate by addition of  
80 binder liquid to form granules (Suresh et al., 2017). WG process is used to enhance flow properties of  
81 powder mixtures, prevent segregation and caking of powders during downstream processing and  
82 storage, and reduce dust during manufacturing (Liu et al., 2021). Size distribution, porosity, and drug  
83 content uniformity are critical attributes of granules and may be monitored and controlled during WG  
84 processes (Meng et al., 2016). Generally, a WG process involves three steps. The first step is wetting of  
85 powder particles by addition of binder liquid to form initial small granules called “nuclei” in a process  
86 called “nucleation” (Hapgood et al., 2003). Nucleation generally occurs via two mechanisms, depending  
87 on particle size distribution (PSD) of powder, droplet size of binder liquid, and wettability of powders  
88 (Muthancheri and Ramachandran, 2020). This nucleation may occur through either “distribution without  
89 spreading” or “immersion with spreading” mechanisms (Muthancheri and Ramachandran, 2020). The  
90 second step includes aggregation of nuclei to form loosely packed and partially saturated granules or  
91 agglomerates that undergo densification and deformation by shear applied to squeeze trapped liquid to  
92 surface of nuclei in a process called “consolidation” (Liu et al., 2000). These saturated granules grow in  
93 size as they aggregate with other granules and powder particles in a process called “layering” (Iveson et  
94 al., 2001b). The third step is attrition and breakage of large granules due to shearing forces applied by  
95 chopper in high shear granulators (HSG) or shearing elements of twin-screw granulators (TSG). Breakage  
96 generally occurs after granules achieve particular size, which is controlled by formulation attributes,  
97 process parameters, and dynamics of granulator used (Iveson et al., 2001a). This attrition process  
98 controls the particle size distribution and aids in distribution of binder liquid (Iveson et al., 2001a).

99 Traditionally, HSG has been used in batch-mode WG at which powders are introduced into a bowl, and  
100 the impeller in the bowl aids in mixing all components. Nuclei particles are formed as the binder liquid is  
101 introduced into bowl. Generally, the granulation process is continued for a certain period after  
102 completion of liquid addition (wet massing time) to allow for granule growth. The chopper aids in  
103 granule breakage and limits formation of oversized granules. Various studies have investigated the  
104 effects of process parameters of HSG on granule characteristics (Alsulays et al., 2018). Impeller speed,  
105 binder liquid spray rate, granulation time, liquid to solid ratio, and chopping are the most critical  
106 parameters reported that may affect quality attributes of granules.

107 Over the past decade, focus has shifted from batch to continuous powder processing to improve  
108 production efficiency, mitigate scale-up issues, and achieve automated real-time monitoring and control  
109 over quality attributes of intermediate and finished products. For this purpose, TSG has been integrated  
110 in continuous manufacturing lines due to its flexibility in the selection of screw type and configuration  
111 (flexible arrangement of conveying, mixing, kneading, and sizing elements), as well as its versatility in  
112 attaching to other unit operations (e.g., feeders and pumps) at different zones of the granulation tunnel  
113 to modify mean residence time of granules. Unlike HSG process, the granulation steps in TSG are  
114 spatially separated and occur in a very short time (El Hagrasy and Litster, 2013). Wetting of powders and  
115 nuclei formation occurs in the vicinity of liquid addition port “nucleation zone”. Conveying elements are  
116 generally used in nucleation zone for transporting the nuclei into the kneading/mixing zone of either  
117 staggered kneading elements, comb-mixing elements, or a combination of both (Dhenge et al., 2012). In  
118 kneading zone, the nuclei undergo granule consolidation and growth. Depending on formulation  
119 attributes and screw parameters of kneading zone (number of kneading elements, staggering angle, and  
120 number of kneading zones per screw), this zone governs breakage and attrition of large agglomerates  
121 (Suresh et al., 2017). Conveying elements are located after kneading zone to transport granules to the  
122 sizing zone prior to exiting. Sizing elements may be employed at the end of the screw to control particle  
123 size distribution of the granulation (Vercruyssen et al., 2015). Despite the advantages of TSG in

124 continuous manufacturing, it may produce granules of broad and multimodal granule size distribution  
125 (GSD) depending on the screw configuration employed (El Hagrasy et al., 2013).

126 Prior to optimizing a TSG step, the complex interplay of formulation and process parameters on the  
127 performance characteristics of the granules requires an identification of operating space in a screening  
128 step based on the past experience and background knowledge. The available screening and optimization  
129 studies investigated mostly immediate release rather than extended release (ER) formulations (Beer et  
130 al., 2014). There is a scarce information on processing ER formulation in TSG and switching from batch  
131 to continuous operation. Higher polymer content of ER formulations may contribute to the failure  
132 modes of TSG process due to premature consolidation, excessive swelling, poor cohesion, and increased  
133 torque, among others. Some of these failure modes may not be observed when the critical  
134 physicochemical characteristics of the granulation of HSG are used as references for switching to  
135 continuous processing of TSG. Therefore, understanding effects of granulation parameters of HSG may  
136 be carried out as a screening step with the goal to mitigate these failure modes when switched to TSG  
137 processing. For example, investigating effects of changing the method of binder addition, namely wet  
138 binder addition (in the liquid phase of granulation) and dry binder addition (as extragranular powder  
139 before compression), on the critical physicochemical characteristics of the granulation may guide the  
140 switch to continuous mode of TSG to limit polymer swelling in granulation tunnel. Other processing  
141 parameters may also be transferred from HSG such as feeding rate of binder liquid, liquid to solid ratio,  
142 and shearing rate by the impeller and chopper speed to TSG. However, operating ranges of these  
143 parameters are narrowed when controlled release polymers with high wet viscosity are used in ER  
144 formulation (Kim et al., 2017). The objective of the current study was to identify the critical  
145 physicochemical characteristics of the granules that may guide the switching of manufacturing of an ER  
146 formulation of metoprolol succinate (a model API) from batch to continuous operation through a  
147 performance-based approach. The effects of processing parameters of HSG process in batch mode on  
148 these critical granulation characteristics were evaluated for this purpose. Translation of these processing  
149 parameters to those of TSG was performed through matching their effects on the performance  
150 characteristics of the granules and of the tablets thus produced.

151

## 152 **Materials and Methods**

153 Metoprolol Succinate was purchased from Unichem Laboratories Ltd (Mumbai, India). HPMC K100M,  
154 HPC HXF, and HPC HF were purchased from Ashland Global Specialty Chemicals Inc. (San Francisco, CA).  
155 Dicalcium Phosphate was purchased from JRS Pharma (Patterson, NY). Magnesium Stearate, PVP K30,  
156 and HPC 100K were purchased from MilliporeSigma (St. Louis, MO). Milli-Q water (resistivity  
157 18.2 MΩ cm) was used for all formulations and solutions.

158

## 159 **Formulation characteristics**

160 The composition of model metoprolol succinate ER formulation manufactured by HSG process is listed in  
161 Table 1. An extragranular fraction of HPMC K100M was added to achieve the dissolution characteristics  
162 that met the USP acceptance criteria for the metoprolol succinate ER tablets (USP39-NF34, 2015).

163

## 164 **Powder blending**

165 Each raw material was passed through sieve #60 and blended in a Turbula blender (WAB group, Old  
166 Bridge, NJ) for 10 minutes. After initial blending, de-lumping was performed by passing mixtures  
167 through sieve #60 before blending again for 5 minutes.

168

#### 169 **Batch operation: granulation in high shear granulator**

170 Batch granulation was carried out in a laboratory scale HSG (Key KG-5 HSG equipped with KG3 bowl, Key  
171 International, Cranbury, NJ). The processing parameters of HSG, blending, and tableting used for  
172 manufacturing of granules and tablets are also listed in Table 1. PVP K30 (5% w/w) was dissolved in  
173 water and used as binder liquid at a solid to liquid ratio (L/S) of 40%. The chopper speed was fixed for all  
174 runs at 4000 rpm. The granules were dried in an open tray oven at 40 °C for 24 hr to a residual moisture  
175 content below 3% w/w (Loss-on-Drying). The dried granules were milled in a Quadro Comil U5 (Quadro  
176 Engineering Corp, Westwood, MA) equipped with a screen of size 1397 µm at 3000 rpm for 10 min.  
177 Milled granules were fractionated using a set of sieves to separate granules fraction of 180-850 µm size  
178 for further downstream processing.

179

#### 180 **Experimental design for batch granulation in HSG**

181 To identify critical performance characteristics of the granules that can achieve targeted dissolution  
182 characteristics, central composite design (CCD) was employed to study effects of varying HSG process  
183 parameters on the granule characteristics. The processing parameters of HSG included impeller speed,  
184 granulation time, and feeding rate of binder liquid. Three replicates of the center point were included  
185 and an orthogonal axial value of 1.287 was used in CCD. The process parameters and their levels  
186 employed in the CCD are described in Table 2. A total of 17 granulation runs (B1-B17) were performed  
187 and analyzed by the least square fit module of JMP software (JMP 12.2.1, SAS Institute Inc., Cary, NC).  
188 The output parameters of granules characteristics included particle size distribution, conditional bulk  
189 density (g/mL, CBD), compressibility (%), CPS) at a consolidation stress of 15 kPa, and cohesion and flow  
190 factor at 3 kPa and 9 kPa.

191

#### 192 **Optimization of processing parameters of HSG**

193 A two-step optimization was performed to obtain a set of optimal values of impeller speed, granulation  
194 time, and spray rate of binder liquid that can achieve the targeted ER dissolution characteristics of  
195 metoprolol succinate. This dissolution characteristics was compared against the USP acceptance criteria  
196 for metoprolol succinate ER tablets (USP39-NF34, 2015). In the first step, the processing parameters of  
197 HSG were optimized to determine an optimal range of CBD and CPS of granules as responses of the  
198 model fitting. In the second step, optimized CBD and CPS values of the granules were used in the model  
199 fitting as independent variables to achieve the target dissolution profile. A generalized desirability  
200 function of JMP was used in both steps of optimization. The desirability function was validated by  
201 preparing a fresh batch of the granules using the optimized operating parameters of HSG followed by  
202 compression into tablets. The predicted characteristics of the granules and tablets were compared to  
203 the corresponding actual characteristics and tested for significance of difference using unpaired t-test  
204 (Liu et al., 2017).

205

#### 206 **Continuous operation: granulation in twin screw granulator**

207 The ConsiGma™ system was used for continuous processing of the same formulation that  
 208 achieved the targeted ER dissolution characteristics of metoprolol succinate. This system has a  
 209 length (L)-to-diameter (D) ratio of 20:1 of the granulation tunnel without a die plate (ConsiGma™-1, GEA  
 210 Process Engineering, Belgium). The ConsiGma 1 system is fitted with a loss-in-weight feeder for  
 211 charging powder blends. The screw configuration consists of 2 kneading zones, each consisting of 4  
 212 kneading elements (L = D/4 for each kneading element) arranged at a staggering angle of 60° “forward”,  
 213 separated by a conveying element (L = 1.5D). Three sizing elements (L = 1.5D) were included at the end  
 214 of twin screw. The other part of twin screw was composed of conveying elements (L = 1.5D). Same  
 215 screw configuration was used in all TSG experiments. The TSG granulation process parameters were  
 216 derived from the optimized HSG granulation parameters. These TSG granulation parameters and screw  
 217 configuration are listed in Table 3 and Figure 1, respectively. The binder liquid was pumped at position 1  
 218 of the granulation tunnel with the help of a peristaltic pump with silicon tubes (internal and external  
 219 diameter of 2.4 and 6.2 mm, respectively) connected to 1.6 mm nozzles. In the granulation process,  
 220 torque on the screw was recorded for process assessment. Same granulation parameters, except screw  
 221 speed, were used for all experiments. Screw speed was varied from 200 rpm to 800 rpm over 4 levels  
 222 (Table 3). Granules produced from TSG runs were collected and dried at 40 °C in an open tray oven for  
 223 24 h to a residual moisture content below 3% w/w (Loss-on-Drying). Before tableting, the dried granules  
 224 were processed for tableting in the same manner as the granules produced by HSG.

225

226 **Characterization of granules**

227 Particle size distribution analysis was carried out using Ro-Tap 30 sieve shaker (W.S. Tyler, Mentor, OH).  
 228 Granules samples of 100 g were sieved for 5 min at an amplitude of 2 mm using a stack of sieves with  
 229 cutoff of 2000, 1400, 1000, 850, 500, 300, and 180 µm. The weight of granules retained on each sieve  
 230 was determined and expressed as percentage (w/w). All granule size distributions were plotted as the  
 231 normalized mass frequency shown in the following equation (Eq. 1) versus the midpoint of each size  
 232 interval (Allen, 2003):

233 
$$f_{mi}(\ln x) = \frac{y_i}{\ln(x_i/x_{i-1})} \dots\dots\dots \text{Eq. 1}$$

234 where  $y_i$  is mass fraction in size interval  $i$  and  $x_i$  is midpoint of each size interval. Percentile values of  
 235 particle size distribution parameters, namely D10, D50, and D90 (particle sizes below 10%, 50%, and 90%  
 236 (w/w) of particles exist, respectively) were determined. Process yield was determined as weight percent  
 237 of particles between 180 and 850 µm. Percent of fine and oversized granules were defined as weight  
 238 percent of particles below 180 µm and greater than 850 µm, respectively.

239 Granule bulk properties, namely CBD and CPS, were measured using FT4 powder rheometer (Freeman  
 240 Technology, Tewkesbury, Gloucestershire, UK). The protocol for the compressibility test on the  
 241 rheometer included conditioning of powder followed by stepwise application of normal stress. Powder  
 242 sample was filled into the measuring vessel and was adjusted to the specified volume. Weight of the  
 243 powder was recorded after one conditioning cycle and splitting a 25 mm/10 mL vessel. CBD (g/mL) was  
 244 then calculated by dividing weight by volume of the sample. The conditioning process included a gentle  
 245 displacement of whole sample by loosening and reaerating the powder bed so that any pre-compaction  
 246 and excess air were removed. CPS of granules was determined by transferring a specified weight of  
 247 granules manually to the measuring vessel of FT4 powder rheometer (Freeman Technology,  
 248 Tewkesbury, Gloucestershire, UK). Two conditioning cycles were applied followed by splitting a 25  
 249 mm/10 mL sample and carefully removing the excess material. Mass of the sample remaining in the  
 250 measuring vessel was then recorded. The blade was replaced with a vented piston that fits the diameter

251 of measuring vessel. A stress was applied to the sample in a range of 0.5 to 15 kPa. CPS was then  
252 calculated from the change in volume after each compression cycle (Macho et al., 2021). CPS at 15 kPa  
253 was used for the optimization study.

254 Flow properties of granules such as unconfined yield strength (UYS), major principal stress (MPS), angle  
255 of internal friction (AIF), flow factor (FF), and cohesion were also measured using the shear cell module  
256 of FT4 powder rheometer (Freeman Technology, Tewkesbury, Gloucestershire, UK). Similar shear cell  
257 assembly to that used in CPS measurement was used. Flow properties were determined by applying pre-  
258 consolidation stress at preshear of 3 and 9 kPa. The shear test consisted of three steps, namely shear  
259 head pre-consolidation, preshear until steady state achieved, and shear test measurement (Macho et  
260 al., 2021). The preshear was applied after each shear measurement to achieve steady state shear stress  
261 and shearing processes. Yield locus was generated from normal and shear stress points. Mohr circle  
262 analysis was used to calculate the abovementioned flow parameters. The FF was calculated using the  
263 following equation (Eq. 2) (Worku et al., 2017):

$$FF = MPS/UYS \dots\dots\dots \text{Eq.2}$$

265

### 266 **Preparation of tablets**

267 Milled granules were fractionated using a set of sieves to separate granules fraction of 180-850 µm size.  
268 This fraction was blended with extragranular fraction of HPMC K100M (particle size < 250µm). The blend  
269 was lubricated for one minute with 1% magnesium stearate and compressed into 10 mm flat round  
270 tablets (250 mg) using Piccola B-10 rotary press (SMI Incorporated, Lebanon, New Jersey).

271

### 272 **Characterization of tablets**

273 The tablets were characterized for breaking strength, weight variation, and dissolution properties. For  
274 measuring breaking strength, ten random tablets per batch were tested using a Pharma test tablet  
275 hardness tester (Pharma Test Apparatebau AG, Hainburg, Germany). Tablet weight variation was  
276 evaluated by weighing **ten random tablets per batch** on a benchtop analytical balance. Dissolution  
277 testing was performed for six random chosen tablets per batch using USP dissolution apparatus II as  
278 described in the USP monograph of metoprolol succinate ER tablets (USP39-NF34, 2015). 900 mL of  
279 phosphate buffer saline (pH 6.8) was used as the dissolution medium and was maintained at 37 °C.  
280 Paddle speed was set at 50 rpm. Aliquots of 2 mL were collected using an autosampler at 1h, 4h, 8h,  
281 14h, and 20h. Quantitation of metoprolol succinate was done using HPLC.

282

### 283 **Chromatographic analysis**

284 Concentrations of metoprolol in dissolution media were determined per the chromatographic method  
285 stated in USP monographs with minor modifications (USP39-NF34, 2015). An HPLC system (Agilent 1260  
286 series, Agilent Technologies, Santa Clara, CA) equipped with a quaternary pump, online degasser,  
287 column heater, autosampler and UV/Vis detector was used. A reversed phase C18 column (Luna, 2.6  
288 µm, 4.6 × 150 mm, Phenomenex Co., Torrance, CA, USA) and C18(2) guard cartridge (5 µm, 4.6 × 12.5  
289 mm) were used. Chromatographic separation was achieved by isocratic elution with a mobile phase  
290 containing phosphate buffer (20 mM of pH 6.8) and acetonitrile (3:2, v/v) at a rate of 1.5 mL/min.  
291 Column temperature was maintained at 35 °C in a column oven, and auto-sampler temperature was  
292 maintained at 20 °C. The injection volume was 10 µL and detection was done by UV at 240 nm.

293 Chemstation software (Agilent Technologies, Santa Clara, CA) was used for data collection and  
294 integration of the chromatographic peaks.

295

## 296 **Statistical analysis**

297 All experiments were performed with 3 or 6 replicates and expressed as the mean  $\pm$  standard deviation.  
298 One-way analysis of variance (ANOVA) followed by multiple comparisons Tukey test was used to  
299 substantiate statistical differences between groups. Results with  $P < 0.05$  were significant.

300

## 301 **Results and discussion**

### 302 **Formulation characteristics**

303 The result in Figure 2 describes the dissolution characteristics of metoprolol succinate from the ER  
304 formulation described in Table 1. These dissolution characteristics met the acceptance criteria listed in  
305 the USP monograph of metoprolol succinate ER tablets (USP39-NF34, 2015). Therefore, this formulation  
306 was used in evaluating the effects of HSG process parameters on the critical granule characteristics and  
307 further switch to continuous granulation. It is worth noting that addition of extragranular fraction of  
308 HPMC K100M (10% w/w) in the tablet formulation resulted in retardation of metoprolol dissolution due  
309 to the formation of a dissolution barrier around the granules by the external layer of dry HPMC K100M  
310 that slowed down the drug dissolution (Roy et al., 2013). Presence of dicalcium phosphate, a  
311 hydrophobic insoluble filler, in the formulation resulted in slow swelling of the hydrophilic matrix and  
312 facilitated erosion of the tablets (Goswami et al., 2014). The use of PVP K30 in the formulation caused  
313 slow diffusion of metoprolol from the tablet matrix by formation of strongly bound clusters in the tablet  
314 core and limited the access of dissolution medium for drug diffusion (Kasperek et al., 2016).

315

### 316 **Size distribution of the granules**

317 Per the CCD in Table 2, seventeen granulation runs were prepared using this ER formulation and the  
318 operating space identified. The results in Figure 3 shows particle size distribution curves of  
319 representative granulation runs per the CCD before and after milling. All granulations exhibited  
320 multimodal particle size distribution. Milling the granules resulted in a transition from multimodal to  
321 unimodal particle size distribution. Variations in the processing parameters of HSG resulted in variation  
322 of particle size distribution parameters (D10, D50, D90) after milling, and percent of fines, oversize, and  
323 yield of granules. For example, D10, D50, and D90 for these 17 granulations varied from 195  $\mu\text{m}$  to 285  
324  $\mu\text{m}$ , from 720  $\mu\text{m}$  to 875  $\mu\text{m}$ , and from 1390  $\mu\text{m}$  to 2200  $\mu\text{m}$  respectively. The percent of fine, oversize  
325 and yield of these granulations varied also from 6.77% to 12.61%, from 1.27% to 13.08%, and from 42%  
326 to 69.66 %, respectively.

327 Statistical analysis of particle size distribution data using least square regression equations of CCD  
328 showed correlations of the process variables with particle size distribution parameters. Impeller speed  
329 was the most significant variable affecting all particle size distribution parameters followed by  
330 granulation time and spray rate of binder liquid. Increasing impeller speed and granulation time while  
331 decreasing spray rate of binder liquid resulted in higher yield percent from granulation runs. This  
332 increase in yield percent could be attributed to an increase in frequency of collision among the granules  
333 (Kotamarthy et al., 2020). The percent of oversize granules increased by decreasing the impeller speed  
334 and granulation time while increasing the spray rate of binder liquid. High spray rate of binder liquid

335 caused inhomogeneous mixing of the binder, formation of lumps, and poor granulation (Sarkar and  
336 Chaudhuri, 2018).

337 Interestingly, impeller speed had a significant positive effect on percent of fines. The increase in collision  
338 velocity and magnitude of forces acting on the granules at higher impeller speed may explain this result  
339 (Oulahna et al., 2003). Granulation time and spray rate did not have significant effects on percent of  
340 fines. Therefore, it was postulated that a uniform particle size distribution of the granules can be  
341 obtained by employing high impeller speed and long granulation time while spraying the binder liquid at  
342 low rates. Table 4 list the desirability functions for optimization particle size distribution parameters.  
343 The maximized desirability revealed the optimum levels for impeller speed, granulation time, and spray  
344 rate of binder liquid at 315 rpm, 5 minutes, and 30 g/min, respectively. Under these optimized  
345 granulation parameters, the predicted fines, oversized, and yield fractions were 8.48%, 2.05%, and  
346 62.21%, respectively. Non-significant differences ( $p < 0.05$ ) were observed among predicted and  
347 observed values of these particle size distribution parameters.

348

#### 349 **Bulk properties of the granules**

350 The results in Figure 4A shows the CBD and CPS of all the granulation runs performed. The CBD of  
351 granulation runs B1-B10 ranged from 0.4 to 0.5 g/mL while the CBD of granulation runs B11-B17 were  
352 significantly higher and ranged from 0.75 and 0.82 g/mL. On the other hand, CPS did not exhibit any  
353 trend among all granulation runs and ranged from 6.3 to 9.6 %.

354 The Figures 4B and 4C show the effects of granulation time on CBD and CPS. The granulation time was  
355 found to affect the CBD and CPS of granulations significantly (Prob>[t] of 0.0134). A direct correlation  
356 between granulation time and CBD was observed. On the other hand, CPS of granulations at a  
357 consolidation stress of 15 kPa was found to decrease significantly (Prob>[t] of 0.0050) by increasing the  
358 granulation time. These results may be attributed to the longer wet massing time for particles to  
359 consolidate and form dense granules (Gabbott et al., 2016). These dense granules achieved greater  
360 packing in the consolidation vessel of the rheometer that resulted in less movement as consolidation  
361 stress was applied.

362 The results in Figure 4B show that spray rate of binder liquid did not significantly affect bulk properties  
363 of the granulations; however, the highest CBD of the granules (1.05 g/mL) was attained at the longest  
364 granulation time of 5.4 min and at a high spray rate of binder liquid of 75 g/min. As demonstrated  
365 earlier, the increase in spray rate resulted in significant increase in oversize fraction of granules that led  
366 to wide granule size distribution and an increase in CBD due to enhanced packing of the granules.

367 The Impeller speed showed a significant quadratic effect (Prob>[t] of 0.0106) on CPS rather than CBD of  
368 the granules. The highest CPS of 12.3% was attained at a lower impeller speed of 150 rpm and shorter  
369 granulation time of 1.5 min (Figure 4C). The lower impeller speed and short granulation time decreased  
370 consolidation and aggregation of the particles during granulation because of limited deformation and  
371 availability of liquid at surface of granules (Iveson et al., 2001b). This ultimately leads to the formation of  
372 granules of low CBD which in turn results in higher compressibility with wide size distribution (Badawy  
373 et al., 2000).

374

#### 375 **Flow properties of the granules**

376 The flow parameters of the granulations were measured by employing Mohr circle analysis of the  
377 relationship between the normal and shear stresses (Carson and Wilms, 2006). For all flow parameters

378 studied, the goodness of fit value for prediction ( $R^2$ ) and the probability value for t-statistic of the data  
379 (p-value) were poor when a consolidation stress of 9 kPa was applied (data not shown). This poor fit  
380 may be attributed to the high deformability of the granules, formation of agglomerates, and sticking at 9  
381 kPa. Therefore, flow characteristics of the granules at a normal stress of 3 kPa were only discussed.

382 The values of UYS and MPS represented stress state of the granules during consolidation. UYS and MPS  
383 of the granules ranged from 0.59 (granulation B1) to 1.36 kPa (granulation B6) and from 6.77  
384 (granulation B1) to 7.45 kPa (granulation B6), respectively. The combined effects of UYS and MPS  
385 resulted in FF of the granules that ranged from 11.5 (granulation B1) and 20.92 (granulation B16). AIF  
386 determined the internal friction among the granules in the shear plane and their ability to withstand the  
387 shear stress applied. It represents the angle between the normal and shear force in the linearized yield  
388 locus. AIF of the granules ranged from 36.5° (granulation B4) to 43.7° (granulation B1).

389 Cohesion among the granules determined the minimum shear stress required in the shear cell to slip the  
390 top layer of powder/granules at zero normal stress. Unlike measurement of other flow parameters, the  
391 direct measurement of cohesion of the granules avoided experimental errors due to packing or  
392 compounding the granules during preparation for the test. The dimensionless cohesion number recently  
393 introduced by Wang and coworkers was then used in the current study to compare the cohesion of the  
394 granules (Wang et al., 2016). This dimensionless cohesion number is the ratio between cohesion and  
395 initial consolidation stress used in the test. Wang et al. classified flow properties of powders based on  
396 this cohesion number as: free flowing powder of cohesion below 0.048, easy flowing powder of  
397 cohesion between 0.048 and 0.121, cohesive powder of cohesion between 0.121 and 0.242, and very  
398 cohesive non-flowing powder of cohesion more than 0.242. Cohesion number of the granules prepared  
399 in the current study ranged from 0.04 (granulation B1) to 0.33 (granulation B6). Based on flow  
400 classification by Wang et al., these granules prepared can be clustered as: granulations B1 and B2 are  
401 free flowing granules, granulations B17, B10, and B15 are easy flowing granules, granulations B8, B9,  
402 B11, B13, B12, B5, B2, and B3 are cohesive granules, and granulations B14, B4, B7, and B6 are non-  
403 flowing granules. This ranking agreed with the FF values determined and showed that cohesion has an  
404 inverse power-law correlation with FF (Figure 5A).

405 The granulation time affected significantly UYS, MPS, and FF of the granules with Prob>[t] values of  
406 0.0139, 0.0050, and 0.0152, respectively. The increase in granulation time resulted in a decrease in both  
407 UYS and MPS while increasing FF of the granules. The results in Figure 5B show a significant positive  
408 interaction between granulation time and impeller speed and its effects on FF and AIF. On the other  
409 hand, this interaction of granulation time and impeller speed was significant and inversely affected the  
410 cohesion of the granules. At a short granulation time of 2 min, the effects of impeller speed on UYS, FF,  
411 and cohesion disappeared; however, this interaction did not affect the MPS (Figure 5B). These results  
412 agreed with particle size distribution, CBD, and CPS data collected that indicated a reduction of CPS, an  
413 increase in CBD and a narrow particle size distribution by increasing the granulation time and impeller  
414 speed to produce more spherical granules with improved flowability (Thapa et al., 2019).

415

#### 416 **Weight uniformity and breaking strength of the tablets**

417 The weight variation data of tablets of all granulations indicated that compression of all granulation runs  
418 resulted in tablets of uniform weight (data not shown). These results indicated that flow properties of  
419 the granules did not affect die filling at the employed compression speed of lab scale. It is noteworthy  
420 that the flow properties of lubricated blend of granules with the extragranular fraction governed the  
421 overall flowability and die filling properties to form tablets of uniform weight. Nonetheless, studying

422 flow properties of the granules in the current study was considered critical for switching the batch  
423 granulation process to a continuous granulation process.

424 The results in Figure 6 shows response surface and interaction plots of the effects of granulation time  
425 and impeller speed of the high shear granulator, and CBD and CPS of the granules on the breaking  
426 strength of the tablets. The breaking strength of the tablets ranged from 3.72 kp (granulation B16) to  
427 5.31 kp (granulation B1). The regression results showed that both granulation time and impeller speed  
428 had significant negative effects on the breaking strength of the tablets with Prob>[t] values of 0.0003  
429 and 0.0001, respectively (Figure 6A). The effect of the impeller speed on the breaking strength of tablets  
430 was more pronounced when longer granulation time was used in HSG indicating a significant negative  
431 interaction (Prob>[t] values of 0.0030) (Figure 6B). The combined effects of granulation time and  
432 impeller speed on breaking strength may be attributed to the enhanced densification and hence lower  
433 compressibility of the granules attained when longer granulation time and faster impeller speed was  
434 used (Figures 4 and 6C). These dense granulations demonstrated a poor packing efficiency that  
435 minimized contact surface area, granule deformation, and inter-granular bonding upon compression (Shi  
436 et al., 2011). Similar results have been reported in literature to indicate that dense granules exhibit  
437 lower porosity and deformability upon compression (Kashani Rahimi et al., 2020).

438

#### 439 **Dissolution properties of the tablets**

440 The drug release from the ER tablets prepared from these granulation runs ranged from 17%  
441 (granulation B17) to 27% (granulation B3) at 1 h; from 40% (granulation B13) to 49% (granulation B7) at  
442 4 h; from 57% (granulation B13) to 69% (granulation B1) at 8 h; from 70% (granulation B13) to 84%  
443 (granulation B3) at 14 h; and from 78% (granulation B13) to 91% (granulation B5) at 20 h. Figure 7A  
444 shows the effects of granulation parameters and bulk properties of the granules, in an ascending order  
445 of p-values, on dissolution of metoprolol tablets after 20 hr. Similar ranking orders were observed for  
446 metoprolol release at earlier time points (1, 4, 8, and 14 hr, data not shown); therefore, dissolution  
447 properties at 20 hr have been discussed below.

448 The results in Figure 7C show that CBD of the granules was the most critical and significant factor  
449 (prob>[t] value of 0.0006) that negatively affected metoprolol dissolution. Granulation time and CPS  
450 showed also significant negative effects on metoprolol dissolution with prob>[t] values of 0.0045 and  
451 0.0060, respectively (Figures 7B). Increasing the impeller speed and spray rate of binder liquid caused a  
452 significant quadratic increase in metoprolol dissolution with prob>[t] values of 0.0106 and 0.0015,  
453 respectively. As shown in previous sections, increasing granulation time and impeller speed resulted in  
454 the formation of dense and less compressible granules which in turn resulted in decreased breaking  
455 strength and metoprolol dissolution properties of their tablets. The results in Figures 7D, 7E, and 7F  
456 confirm these findings through the interaction plots of the effects of bulk properties and tablet breaking  
457 strength on metoprolol dissolution. The interaction plots in Figure 7D clearly demonstrate that the  
458 significant effect of CPS on metoprolol dissolution was more pronounced at higher CBD of the granules  
459 (1.1 g/mL). Similarly, the effect of breaking strength of the tablets on metoprolol dissolution was more  
460 pronounced when granules of the highest CBD (1.1 g/mL) were used for their manufacturing (Figure 7E).  
461 At a high breaking strength of 5.3 kp, the reduction in metoprolol dissolution by increasing CBD of the  
462 granules may be attributed to the plastic deformation of the granules that increased the contact surface  
463 area for bonding during compression. At the highest CBD of 1.01 g/mL, a positive effect of breaking  
464 strength on metoprolol dissolution was observed and may be explained by the minimal effect of  
465 compression pressure to cause deformation of granules and particle to particle bonding (Figure 7F). On  
466 the contrary, this positive effect was not observed by changing breaking strength of the tablets prepared  
467 using granules of low CBD of 0.43 g/mL.

468 It is worth noting that not only critical attributes of the granules governed the metoprolol dissolution,  
469 but the extragranular fraction of HPMC K100M also contributed to the release mechanism. Since same  
470 amount of extragranular HPMC K100M was used for all granulation runs, the dissolution data could not  
471 unveil effects of extragranular components on metoprolol dissolution. Overall, the release mechanism  
472 of metoprolol from these ER tablets relied on the theory of swelling and erosion behaviors of the  
473 extragranular matrix that controls access of the dissolution medium to the granules present in the core  
474 of the tablets. Metoprolol dissolution started by diffusion of the dissolution medium into the glassy  
475 HPMC of the extragranular matrix. As a result, HPMC chains plasticized, and its glass transition  
476 temperature reduced to the ambient temperature. Glassy extragranular HPMC transformed then to a  
477 rubbery gel state (gel layer) that allowed more diffusion of dissolution medium to granules in tablet  
478 core. This gel layer composed of highly concentrated HPMC solution, and metoprolol released through  
479 erosion of this gel layer (erosion front). The solid phase of intragranular HPMC and HPC fractions  
480 compensated the eroded gel layer of the extragranular fraction to form a polymer concentration  
481 gradient around the tablet, starting at a high concentration in the core of dry granules and declining  
482 through the gel layer towards the surface of the extragranular gel layer. Consequently, this theory  
483 indicates that critical attributes of the granules contribute to overall swelling of polymeric contents of  
484 the tablet and further metoprolol dissolution. Therefore, upon using the same extragranular polymeric  
485 fraction, similar dissolution behavior of the drug may be achieved when granules of similar quality  
486 attributes are produced in a continuous granulation process of TSG.

487

#### 488 **Performance characteristics of HSG granulations as a reference for TSG granulation**

489 In view of complex effects of granulation parameters on metoprolol dissolution, an optimization  
490 strategy was followed to obtain a set of optimal impeller speed, granulation time, and spray rate of the  
491 binder liquid. The results in Table 5 lists the optimal HSG parameters and performance characteristics of  
492 the granules and tablets thus obtained. Nonsignificant differences were observed among the predicted  
493 and actual values of these characteristics.

494 The above findings about the effects of HSG granulation parameters on the quality attributes of the  
495 granules guided switching this formulation from batch operation in HSG to continuous operation in TSG.  
496 Tablets were compressed to similar target breaking strength for all granulation runs. Evaluation of the  
497 critical attributes of the granules revealed that successful switch to continuous granulation depended on  
498 the L/S ratio and the extent of shear applied, and particle size distribution of granules within the  
499 operating space selected for this formulation in HSG. For example, the shearing effect of impeller speed  
500 and granulation time in HSG was compared to the shearing effect of the kneading zones and residence  
501 time in TSG to produce granules of similar characteristics. Three mechanisms, namely a) wetting and  
502 nucleation, b) consolidation and growth, and c) breakage and attrition, governed granulation in HSG and  
503 TSG. During spraying of binder liquid in spray zone of HSG bowl, the binder droplets wetted the powder  
504 surface, penetrated powder pores, and formed loose agglomerates or “nuclei”, with limited swelling of  
505 the polymers included in the formulation. These loose agglomerates remained in motion to disperse  
506 binder droplets and to facilitate granule deformation and breakage by chopper action. As the most  
507 significant granulation parameter, increasing the granulation time caused more nucleation,  
508 consolidation, and growth of these agglomerates, while enabling granules deformation and breakage  
509 through collision of granules and chopper action. Under these mechanisms, larger granules decreased in  
510 size while producing dense granules that achieved the targeted dissolution profile of metoprolol from  
511 the ER tablets. The performance characteristics of the granules produced through this granulation  
512 mechanisms of HSG were used as a reference for comparison for the granulation obtained via the  
513 continuous TSG process.

514 **Granulation in twin screw granulator**

515 Preliminary experiments indicated that a lower feeding rate of binder liquid was needed for granulation  
516 in TSG. Compared to granulation in HSG, using the same L/S ratio of 40% caused excessive swelling of  
517 the formulation and led to higher torque in TSG. This excessive swelling occurred due to the limited  
518 space inside the TSG barrel, increased shear, and reduced granulation time in the TSG (Kyttä et al.,  
519 2020). Therefore, a lower L/S ratio of 25% was employed in subsequent TSG runs.

520 The granules produced at various screw speeds (200, 400, 600, and 800 rpm) of TSG after drying  
521 exhibited a multimodal particle size distribution which changed to unimodal after milling (data not  
522 shown), much like the granulation produced by high shear granulation process.

523 The results in Table 6 lists the bulk properties of granules and dissolution profiles of tablets produced by  
524 TSG granulations at screw speeds of 200, 400, 600, and 800 rpm. It is noteworthy that variations in  
525 screw speed did not affect CBD of the granules which varied from 0.599 g/mL - 0.604 g/mL; however,  
526 the CPS of the granules ranged from 11.51% to 14.57%. No specific trends in the bulk properties of the  
527 granules were found as a function of screw speed and within operating space selected. However, these  
528 bulk properties were comparable to those of the reference granules produced by HSG (Figure 4 and  
529 Table 6).

530 The dissolution profile of tablets prepared with TSG granules (Run S4) was found comparable to the  
531 dissolution profile of the reference tablets ( $F_2 > 50$ ) that were prepared with optimized HSG granules.  
532 The dissolution data listed in Table 6 show that screw speed had a more pronounced effect on  
533 metoprolol dissolution. For example, percent of metoprolol released in 20 hr decreased from 94.4% to  
534 80.6% by increasing screw speed of TSG from 200 rpm to 800 rpm (Table 6). This result may be  
535 attributed to the decrease in residence time of the formulation at higher screw speed while exerting an  
536 axial shear mixing by the kneading zones {Lalith Kotamarthy, 2021 #167}. This axial shear mixing  
537 improved granules consolidation and particle-to-particle bonding during tableting.

538 Several failure modes were identified while selecting a screw configuration that can produce  
539 comparable shearing effects on the granulation. Premature consolidation of the blend in the screw  
540 tunnel, excessive swelling of the formulation to form sheets rather than granules, poor cohesion of the  
541 blend due to inconsistent binding and shearing, and formation of threads and deformed granules are  
542 examples of granulation failure modes observed during transfer to continuous granulation (Figure 8).  
543 Therefore, for optimization of the screw configuration and other processing parameters of the TSG, it is  
544 critical to determine the optimum operating space for continuous granulation of this ER formulation.  
545 Further studies are in progress to understand the interactions among the screw configuration and other  
546 operating parameters for manufacturing ER tablets by TSG.

547

548 **Conclusion**

549 For switching the granulation of an ER formulation from the batch mode of HSG to the continuous mode  
550 of TSG, it is necessary first to thoroughly characterize bulk properties of the granules produced via a HSG  
551 process and the dissolution of the resulting tablets. These bulk properties and tablet dissolution may  
552 serve as a reference for comparing granulations and tablets when manufactured using continuous TSG  
553 process. Switching from batch to continuous operation may not be achieved simply by duplicating the  
554 liquid to solid ratio and or the shearing effects in TSG. Instead, effects of screw configuration variables  
555 and their interactions with other operating parameters are critical to achieve the product performance  
556 desired.

557

558 **Acknowledgment**

559 This project was supported in part by an appointment of Lalith Kotamarthy and Pradeep Kumar Bolla to  
560 the Research Participation Program at the CDER/OPQ/OTR of U.S. Food and Drug Administration,  
561 administered by the Oak Ridge Institute for Science and Education through an interagency agreement  
562 between the U.S. Department of Energy and FDA.

563

564 **References**

565 Allen, T., 2003. 2 - Data presentation and interpretation, in: Allen, T. (Ed.), Powder Sampling and Particle  
566 Size Determination. Elsevier, Amsterdam, pp. 56-141.

567 Alsulays, B.B., Fayed, M.H., Alalaiwe, A., Alshahrani, S.M., Alshetaili, A.S., Alshehri, S.M., Alanazi, F.K.,  
568 2018. Mixing of low-dose cohesive drug and overcoming of pre-blending step using a new gentle-wing  
569 high-shear mixer granulator. *Drug Dev Ind Pharm* 44, 1520-1527.

570 Badawy, S.I.F., Menning, M.M., Gorko, M.A., Gilbert, D.L., 2000. Effect of process parameters on  
571 compressibility of granulation manufactured in a high-shear mixer. *International Journal of*  
572 *Pharmaceutics* 198, 51-61.

573 Beer, P., Wilson, D., Huang, Z., De Matas, M., 2014. Transfer from high-shear batch to continuous twin  
574 screw wet granulation: a case study in understanding the relationship between process parameters and  
575 product quality attributes. *Journal of pharmaceutical sciences* 103, 3075-3082.

576 Carson, J.W., Wilms, H., 2006. Development of an international standard for shear testing. *Powder*  
577 *Technol* 167, 1-9.

578 Dhenge, R.M., Cartwright, J.J., Hounslow, M.J., Salman, A.D., 2012. Twin screw granulation: Steps in  
579 granule growth. *International Journal of Pharmaceutics* 438, 20-32.

580 El Hagrasy, A.S., Hennenkamp, J.R., Burke, M.D., Cartwright, J.J., Litster, J.D., 2013. Twin screw wet  
581 granulation: Influence of formulation parameters on granule properties and growth behavior. *Powder*  
582 *Technology* 238, 108-115.

583 El Hagrasy, A.S., Litster, J.D., 2013. Granulation rate processes in the kneading elements of a twin screw  
584 granulator. *AIChE Journal* 59, 4100-4115.

585 Gabbott, I.P., Al Husban, F., Reynolds, G.K., 2016. The combined effect of wet granulation process  
586 parameters and dried granule moisture content on tablet quality attributes. *European Journal of*  
587 *Pharmaceutics and Biopharmaceutics* 106, 70-78.

588 Goswami, K., Khurana, G., Marwaha, R.K., Gupta, M., 2014. Development and evaluation of extended  
589 release ethylcellulose based matrix tablet of diclofenac sodium. *International Journal of Pharmacy and*  
590 *Pharmaceutical Sciences* 6, 296-301.

591 Hapgood, K.P., Litster, J.D., Smith, R., 2003. Nucleation regime map for liquid bound granules. *AIChE*  
592 *Journal* 49, 350-361.

593 Iveson, S.M., Litster, J.D., Hapgood, K., Ennis, B.J., 2001a. Nucleation, growth and breakage phenomena  
594 in agitated wet granulation processes: a review. *Powder Technology* 117, 3-39.

595 Iveson, S.M., Wauters, P.A.L., Forrest, S., Litster, J.D., Meesters, G.M.H., Scarlett, B., 2001b. Growth  
596 regime map for liquid-bound granules: further development and experimental validation. *Powder*  
597 *Technology* 117, 83-97.

598 Kashani Rahimi, S., Paul, S., Sun, C.C., Zhang, F., 2020. The role of the screw profile on granular structure  
599 and mixing efficiency of a high-dose hydrophobic drug formulation during twin screw wet granulation.  
600 *International Journal of Pharmaceutics* 575, 118958.

601 Kasperek, R., Zimmer, L., Zun, M., Dwornicka, D., Wojciechowska, K., Poleszak, E., 2016. The application  
602 of povidone in the preparation of modified release tablets. *Current Issues in Pharmacy and Medical*  
603 *Sciences* 29, 71-78.

604 Kim, S.H., Hwang, K.M., Cho, C.H., Nguyen, T.T., Seok, S.H., Hwang, K.M., Kim, J.Y., Park, C.W., Rhee, Y.S.,  
605 Park, E.S., 2017. Application of continuous twin screw granulation for the metformin hydrochloride  
606 extended release formulation. *Int J Pharm* 529, 410-422.

607 Kotamarthy, L., Metta, N., Ramachandran, R., 2020. Understanding the Effect of Granulation and Milling  
608 Process Parameters on the Quality Attributes of Milled Granules. *Processes* 8, 683.

609 Kytä, K.M., Lakio, S., Wikström, H., Sulemanji, A., Fransson, M., Ketolainen, J., Tajarobi, P., 2020.  
610 Comparison between twin-screw and high-shear granulation - The effect of filler and active  
611 pharmaceutical ingredient on the granule and tablet properties. *Powder Technology* 376, 187-198.

612 Liu, B., Wang, J., Zeng, J., Zhao, L., Wang, Y., Feng, Y., Du, R., 2021. A review of high shear wet  
613 granulation for better process understanding, control and product development. *Powder Technology*  
614 381, 204-223.

615 Liu, H., Galbraith, S.C., Ricart, B., Stanton, C., Smith-Goettler, B., Verdi, L., O'Connor, T., Lee, S., Yoon, S.,  
616 2017. Optimization of critical quality attributes in continuous twin-screw wet granulation via design  
617 space validated with pilot scale experimental data. *International Journal of Pharmaceutics* 525, 249-263.

618 Liu, L.X., Litster, J.D., Iveson, S.M., Ennis, B.J., 2000. Coalescence of deformable granules in wet  
619 granulation processes. 46, 529-539.

620 Macho, O., Gabrišová, L., Brokešová, J., Svačinová, P., Mužíková, J., Galbavá, P., Blaško, J., Šklubalová, Z.,  
621 2021. Systematic study of paracetamol powder mixtures and granules tableability: Key role of  
622 rheological properties and dynamic image analysis. *International Journal of Pharmaceutics* 608, 121110.

623 Meng, W., Kotamarthy, L., Panikar, S., Sen, M., Pradhan, S., Marc, M., Litster, J.D., Muzzio, F.J.,  
624 Ramachandran, R., 2016. Statistical analysis and comparison of a continuous high shear granulator with  
625 a twin screw granulator: Effect of process parameters on critical granule attributes and granulation  
626 mechanisms. *International Journal of Pharmaceutics* 513, 357-375.

627 Muthancheri, I., Ramachandran, R., 2020. Mechanistic understanding of granule growth behavior in bi-  
628 component wet granulation processes with wettability differentials. *Powder Technology* 367, 841-859.

629 Oulahna, D., Cordier, F., Galet, L., Dodds, J.A., 2003. Wet granulation: the effect of shear on granule  
630 properties. *Powder Technology* 130, 238-246.

631 Roy, H., Brahma, C.K., Nandi, S., Parida, K.R., 2013. Formulation and design of sustained release matrix  
632 tablets of metformin hydrochloride: Influence of hypromellose and polyacrylate polymers. *International*  
633 *journal of applied & basic medical research* 3, 55-63.

634 Sarkar, S., Chaudhuri, B., 2018. DEM modeling of high shear wet granulation of a simple system. *Asian*  
635 *Journal of Pharmaceutical Sciences* 13, 220-228.

636 Shi, L., Feng, Y., Sun, C.C., 2011. Massing in high shear wet granulation can simultaneously improve  
637 powder flow and deteriorate powder compaction: A double-edged sword. *European Journal of*  
638 *Pharmaceutical Sciences* 43, 50-56.

639 Suresh, P., Sreedhar, I., Vaidhiswaran, R., Venugopal, A., 2017. A comprehensive review on process and  
640 engineering aspects of pharmaceutical wet granulation. *Chemical Engineering Journal* 328, 785-815.

641 Thapa, P., Choi, D.H., Kim, M.S., Jeong, S.H., 2019. Effects of granulation process variables on the  
642 physical properties of dosage forms by combination of experimental design and principal component  
643 analysis. *Asian Journal of Pharmaceutical Sciences* 14, 287-304.

644 USP39-NF34, 2015. United States Pharmacopeial Convention-U.S. Pharmacopeia National Formulary.  
645 United States Pharmacopeia.

646 Vercruyssen, J., Burggraef, A., Fonteyne, M., Cappuyns, P., Delaet, U., Van Assche, I., De Beer, T.,  
647 Remon, J.P., Vervaet, C., 2015. Impact of screw configuration on the particle size distribution of granules  
648 produced by twin screw granulation. *International Journal of Pharmaceutics* 479, 171-180.

649 Wang, Y., Koynov, S., Glasser, B.J., Muzzio, F.J., 2016. A method to analyze shear cell data of powders  
650 measured under different initial consolidation stresses. *Powder Technology* 294, 105-112.

651 Worku, Z.A., Kumar, D., Gomes, J.V., He, Y., Glennon, B., Ramisetty, K.A., Rasmuson, Å.C., O'Connell, P.,  
652 Gallagher, K.H., Woods, T., Shastri, N.R., Healy, A.-M., 2017. Modelling and understanding powder flow  
653 properties and compactability of selected active pharmaceutical ingredients, excipients and physical  
654 mixtures from critical material properties. *International Journal of Pharmaceutics* 531, 191-204.

655

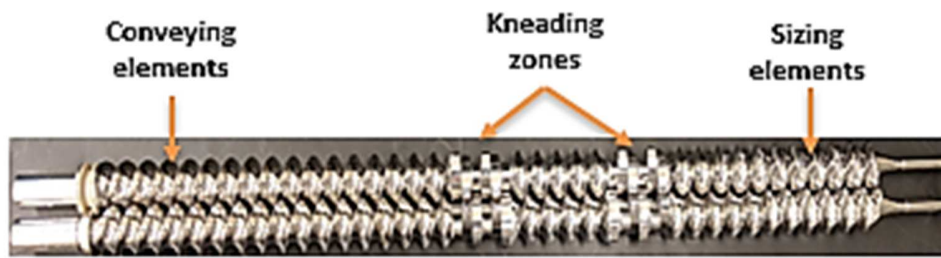


Figure 1: Screw configuration used in twin screw granulation (TSG).

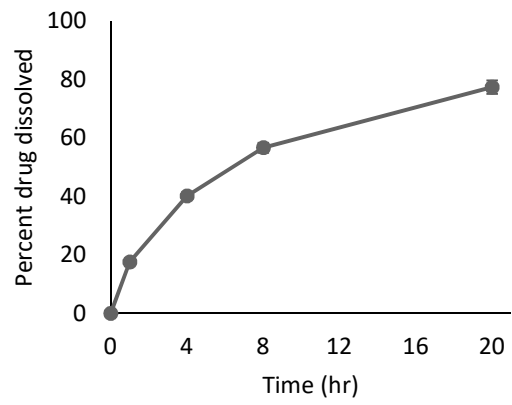


Figure 2: Dissolution profile of metoprolol succinate from the ER formulation described in Table 1 (error bars did not exceed 3% at all points).

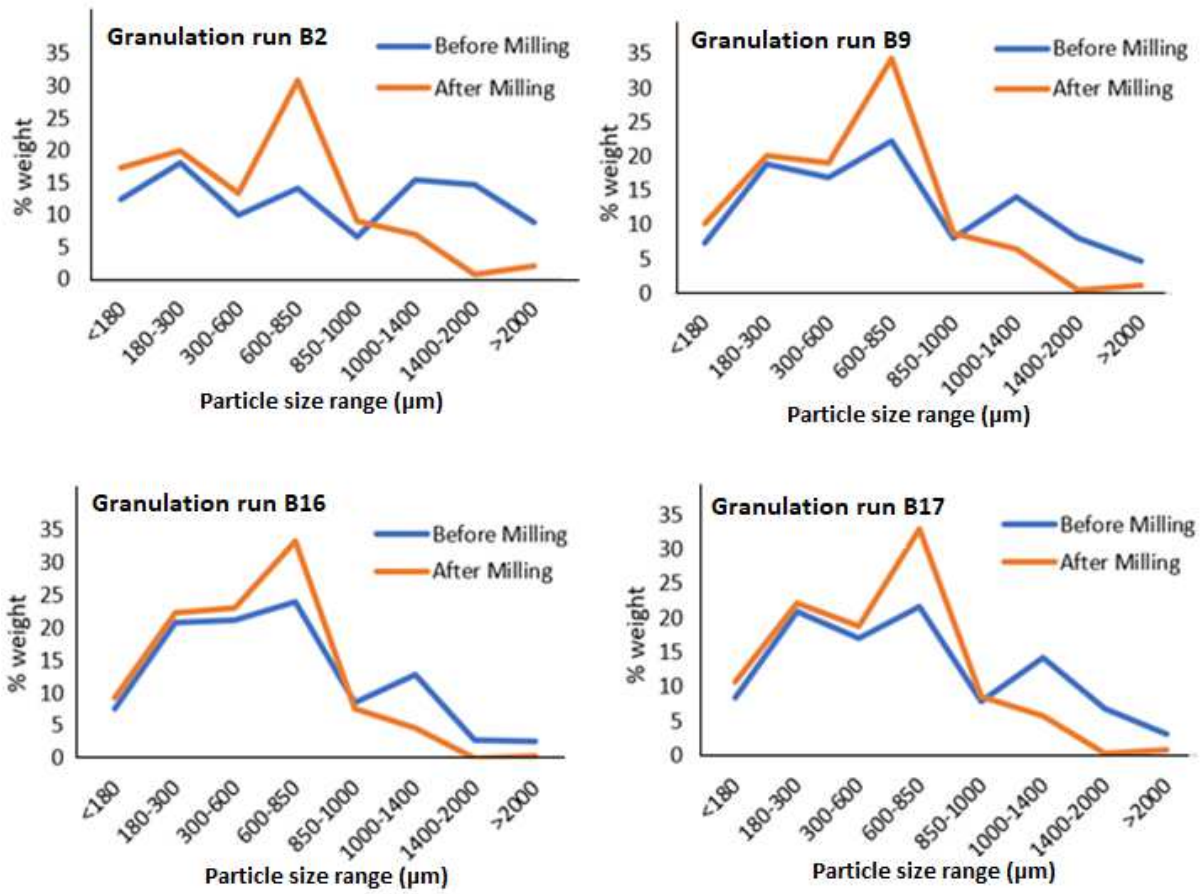


Figure 3: Size distribution curves of representative granulation runs (granulations B2, B9, B16, and B17).

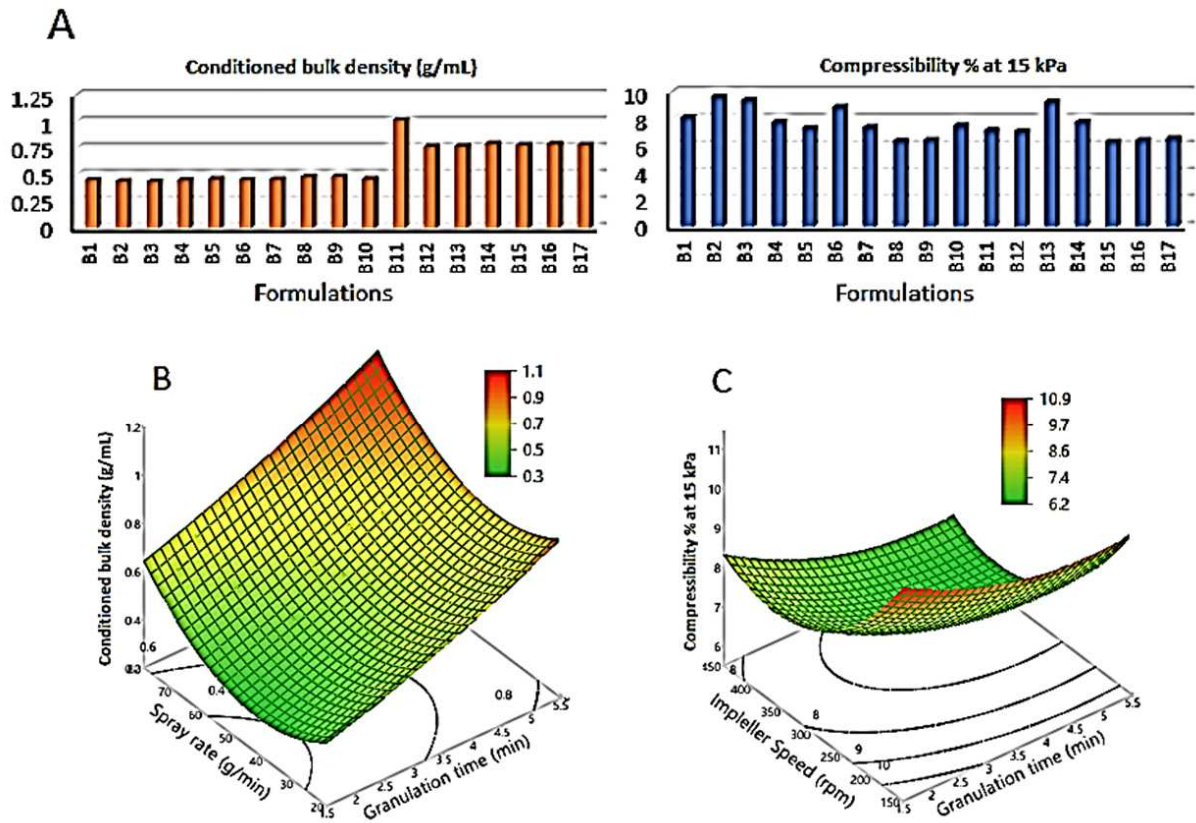


Figure 4: Conditioned bulk density and compressibility of CCD granulations at 15 kPa (A); and response surface and contour plots showing the effects of impeller speed, granulation time, and spray rate of binder liquid on conditioned bulk density (B) and compressibility of the granulations at 15 kPa (C).

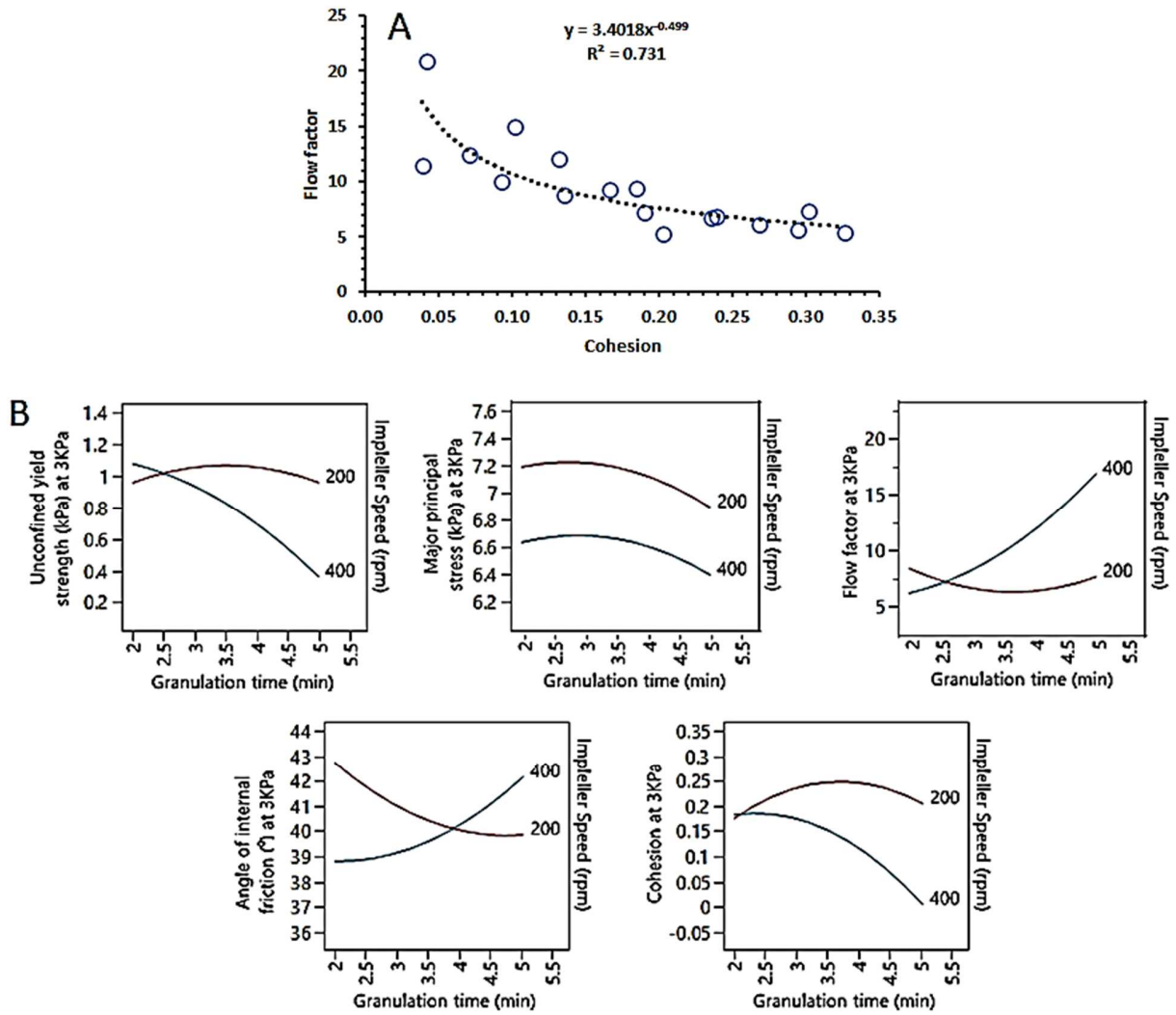


Figure 5: Inverse power-law correlation (A) of cohesion and flow factor of the granules; and Interaction plots (B) of effects of granulation time and impeller speed on unconfined yield strength, major principal stress, flow factor, angle of internal friction, and cohesion of the granules consolidated in the shear cell at 3 kPa stress.

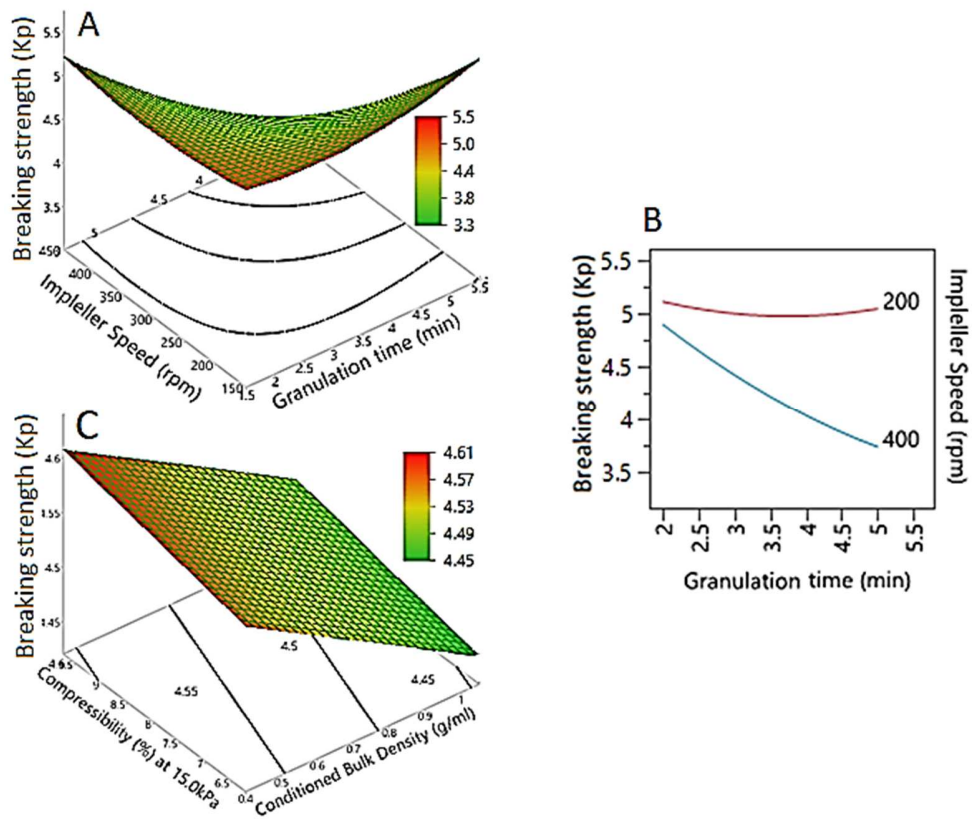


Figure 6: Response surface, contour, and interaction plots of the effects of granulation time and impeller speed (A and B), and effect of conditioned bulk density and compressibility of the granules at 15 kPa on the breaking strength of the tablets (C).

**A**

Term	Estimate	Prob> t
CBD (g/ml)	-14.97	*0.0006
(Spray rate) <sup>2</sup> (g/min)	2.33	*0.0015
Granulation time (min)	-2.98	*0.0045
Compressibility (%) at 15.0kPa	-3.04	*0.0060
(Impeller Speed) <sup>2</sup> (rpm)	2.16	*0.0106
Impeller Speed (rpm)	-2.42	*0.0173
Spray rate (g/min)	0.38	0.2948
Granulation time*Impeller Speed	0.29	0.3431
Impeller Speed*Spray rate	-0.28	0.3867
Granulation time*Spray rate	0.15	0.6086
(Granulation time) <sup>2</sup> (min)	0.17	0.6654

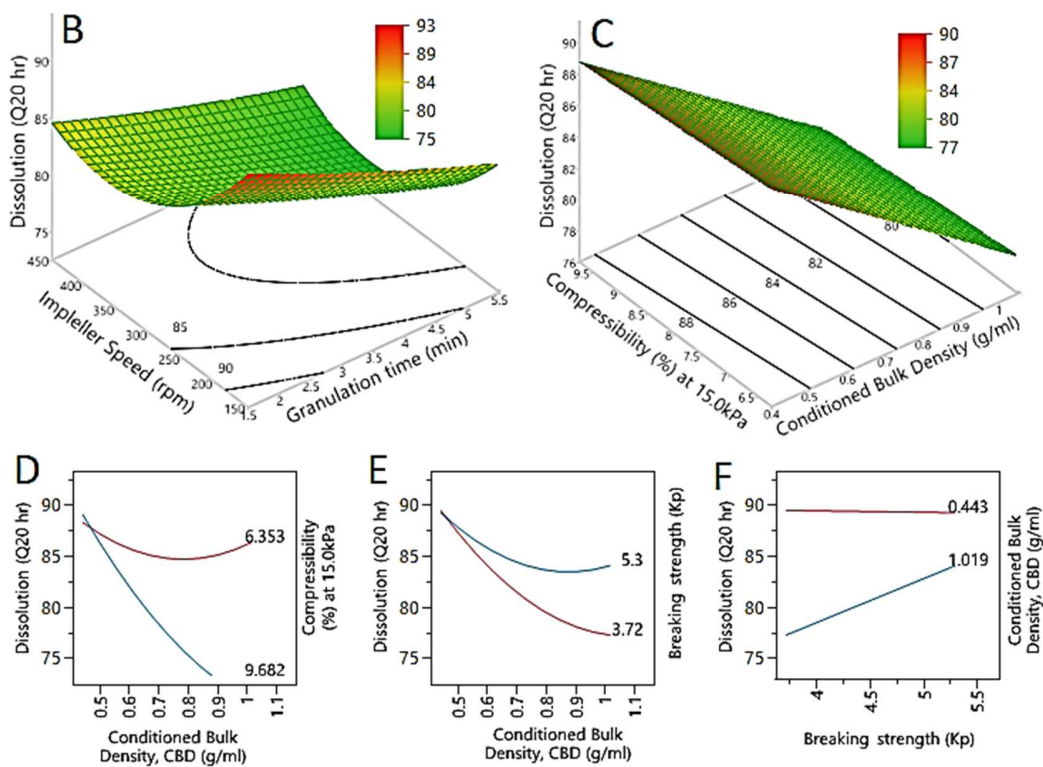


Figure 7: Sorted parameter estimates and Prob>|t| values (A), response surface and contour plots (B and C), and interaction plots (D and E) showing the effects of granulation parameters, granules attributes, and breaking strength of tablets on the dissolution of metoprolol tablets in 20 hrs.

**Premature consolidation**



**Excessive swelling**



**Poor cohesion**



**Threaded granules**

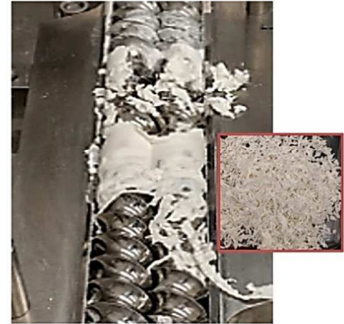


**Figure 8: Examples of failure modes observed during the transfer from batch to continuous granulation**

Table 1: Composition of metoprolol succinate ER formulation and HSG processing parameters

<b>Formulation composition</b>	<b>(%)</b>
Metoprolol Succinate	10
HPMC K100M	25
HPC 100K	20
Dicalcium Phosphate	24
PVP K30	5
Extra-granular HPMC K100M	15
Magnesium stearate	1
<b>HSG Processing parameters</b>	
Blending of excipients	15 minutes
HSG impeller speed	250 rpm
HSG chopper speed	4000 rpm
Binder liquid feed rate	60 g/min
Batch Size	100 g
Mill screen size	1397 $\mu$ m
Mill impeller speed	3000 rpm
Mill time	10 minutes
Lubrication time	30 s
Compression force	17 KN

HPMC is hydroxypropyl methylcellulose; HPC is hydroxypropyl cellulose; and PVP is polyvinyl pyrrolidone.

Table 2: The ranges of Process Parameters employed in the central composite design.

	Impeller Speed (rpm)	Granulation time (min)	Feeding rate of binder liquid (g/min)
<b>Levels of variables</b>			
Low level	200	2	30
Medium Level	300	3.5	50
High Level	400	5	70
<b>Processing parameters used in HSG runs</b>			
B1	300	1.57	50
B2	200	2	30
B3	200	2	70
B4	400	2	30
B5	400	2	70
B6	171.28	3.5	50
B7	300	3.5	24.26
B8 *	300	3.5	50
B9 *	300	3.5	50
B10 *	300	3.5	50
B11	300	3.5	75.74
B12	428.72	3.5	50
B13	200	5	30
B14	200	5	70
B15	400	5	30
B16	400	5	70
B17	300	5.43	50

\* B8, B9 and B10 are three repetitions of the center point.

Table 3. Granulation parameters used for continuous wet granulation.

Batch no	Screw speed (rpm)	Power feed rate (kg/hr)	Liquid feed rate (kg/hr)
<b>C200</b>	200	5	1.25
<b>C400</b>	400		
<b>C600</b>	600		
<b>C800</b>	800		
Solid to liquid ratio (%)		25	
Feed factor (kg/hr)		40.12	
<b>Screw configuration</b>			
Conveying elements		15	
Kneading elements		4 per zone	
Kneading zone		2	
Elements between kneading zones		5	
Staggering angle		60° Forward	
Sizing elements		3	
Zone for liquid feed		Position 1	

Table 4: Desirability parameters and actual values of size distribution parameters of optimized HSG processing parameters.

<b>Properties</b>	<b>High</b>	<b>Medium</b>	<b>Low</b>	<b>Desirability</b>	<b>Optimized predicted values</b>
<b>D10 (µm)</b>	250	225	200	Match target	248.81
<b>D50 (µm)</b>	800	775	750	Match target	758.2
<b>D90 (µm)</b>	1750	1570	1390	Minimize	1587.2
<b>Fines (%)</b>	9	7.75	6.5	Minimize	8.48
<b>Oversize (%)</b>	5	3	1	Minimize	2.05
<b>% Yield (%)</b>	70	66	62	Maximize	62.21

Table 5: The optimized HSG parameters and characteristics of the resulting granules and tablets

<b>Optimized HSG Settings</b>				
Granulation Time	5 minutes			
Impeller Speed	331 rpm			
Spray rate	68.4 g/min			
Chopper Speed (rpm)	4000 rpm			
Liquid/Solid Ratio	40%			
<b>Bulk properties of the granules *</b>	<b>Predicted value</b>	<b>Actual value</b>	<b>Dissolution profiles **</b>	
CBD (g/mL)	0.897	0.797		
CPS (%) at 15 kPa	6.353	6.979		
<b>Tablet Breaking Strength (kp)</b>	4.025	3.98		
<b>Dissolution characteristics</b>				
Dissolution (1 hr)	18.49	18.53		
Dissolution (4 hr)	38.47	42.51		
Dissolution (8 hr)	57.60	61.35		
Dissolution (20 hr)	80.75	86.14		

\* CBD and CPS are conditioned bulk density and compressibility of the granules, respectively.

\*\* Error bars did not exceed 3% at all dissolution point.)

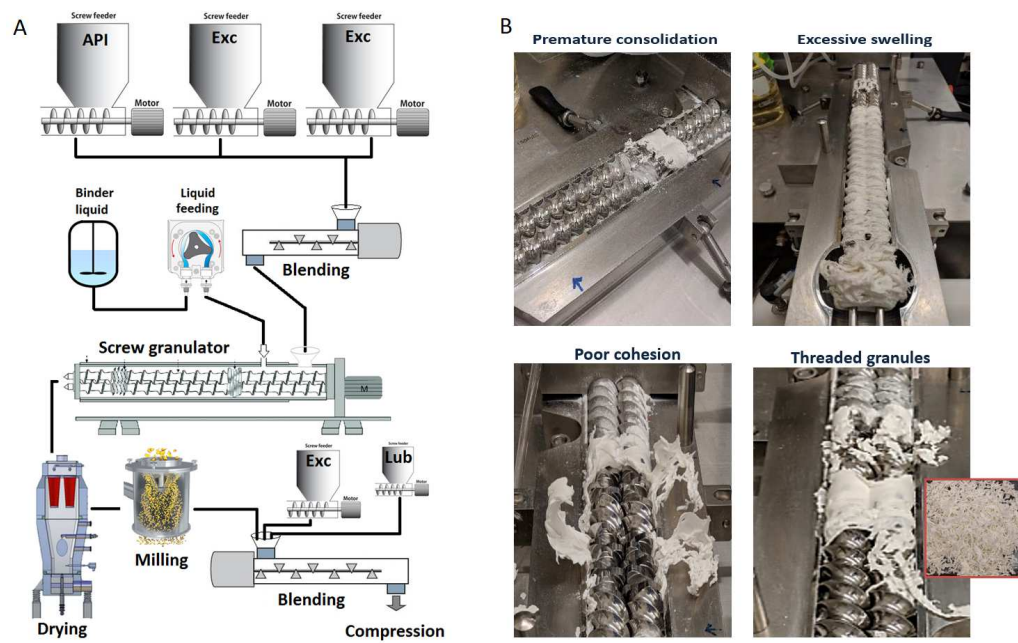
Table 6: Bulk properties of granules and dissolution profiles of tablets produced by continuous wet granulation at various screw speeds.

Run #	Screw speed (rpm)	Bulk properties of the granules *		Dissolution profiles of tablets **
		CBD (g/mL)	CPS (%)	
S1	200	CBD (g/mL)	0.599	<p>Metoprolol released (%)</p> <p>Time (hr)</p> <p>Legend:                      200 rpm (red line with circles)                      400 rpm (grey line with squares)                      600 rpm (yellow line with triangles)                      800 rpm (blue line with diamonds)                 </p>
		CPS (%)	11.51	
S2	400	CBD (g/mL)	0.598	
		CPS (%)	14.57	
S3	600	CBD (g/mL)	0.597	
		CPS (%)	12.77	
S4	800	CBD (g/mL)	0.604	
		CPS (%)	11.68	

\* CBD and CPS are conditioned bulk density and compressibility of the granules, respectively.

\*\* Error bars did not exceed 3% at all dissolution point.)

## Graphical abstract



Process diagram of continuous granulation line of integrated feeding, blending, granulation, milling and drying operations (A); and failure modes (B) observed during continuous granulation.